



Experimental study of air jets pathways in large slot ventilated spaces

**A. Fissore
G. Liébecq
Laboratory of Thermodynamics
University of Liège
Belgium**

D2

66

SLOT VENTILATED SPACES

A. Fissore*, G. Liébecq
 Laboratory of Thermodynamics
 University of Liège
 Belgium

SUMMARY

The ventilation of a sheep-fold is experimentally investigated on a reduced scale model. Though air flows are characteristic of combined wind effects and natural convection due to heat generated from animals, the application is also representative of air flow patterns observed in the ventilation of large industrial halls. The paper describes the experimental facility and presents air flow patterns observed. It discusses the effect of Archimede and Coanda effects on jets pathways and investigates the influence of the length of ventilation slots on the air distribution.

List of Symbols

b_o (m)	:	characteristic length, i.e. width of ventilation slot
F_v (-)	:	ratio of velocities at slot location (always > 1)
l (m)	:	length of slot
L (m)	:	length of wall where slot is located
R (m)	:	curvature radius of jet
SD (m/s)	:	standard deviation on velocity
t (s)	:	time
T (°C)	:	temperature
T_r (°C)	:	reference temperature, i.e. mean temperature of the inside air
TI	:	turbulence intensity at inlets (SD/V_o)
V (m/s)	:	velocity
V_m (m/s)	:	velocity on central line of jet
V_o (m/s)	:	velocity at ventilation slot
β (°C ⁻¹)	:	$1/T_r$
σ	:	standard error
ν (m ² /s)	:	cinematic viscosity

Subscripts

m	:	model or condition on central line of jet
p	:	prototype
c	:	critical
0	:	conditions at ventilation slot
$1,2$:	slots numbering

Dimensionless Numbers

$$Ar = \frac{g \beta (T_r - T_o) b_o}{\nu_o^2}$$

$$Re = \frac{V_o b_o}{\nu}$$

* Present address : Departement of Mechanical Engineering
 University of Concepcion, Chile

Introduction

The indoor climate of industrial halls influences health and work efficiency of human beings. The same applies to homeothermal animals, where the control of air and mean radiant temperature, humidity and air velocities may become critical for their adequate health, growth, productivity and reproduction.

Industrial halls and cattle sheds present further similarities : very often, both types of buildings are long and narrow, with high triangular roofs. They are ventilated (by mechanical means or naturally) through longitudinal slots in one or both lateral walls, while extraction occurs at the vertex of the roof (figure 1).

The main parameters influencing air flow patterns in the occupied zone of such buildings were experimentally identified on a reduced scale model. The experimental sheep - fold of the University was selected as prototype building. The study determined air flow patterns with special emphasis on the location of jets and their interaction in the occupied zone.

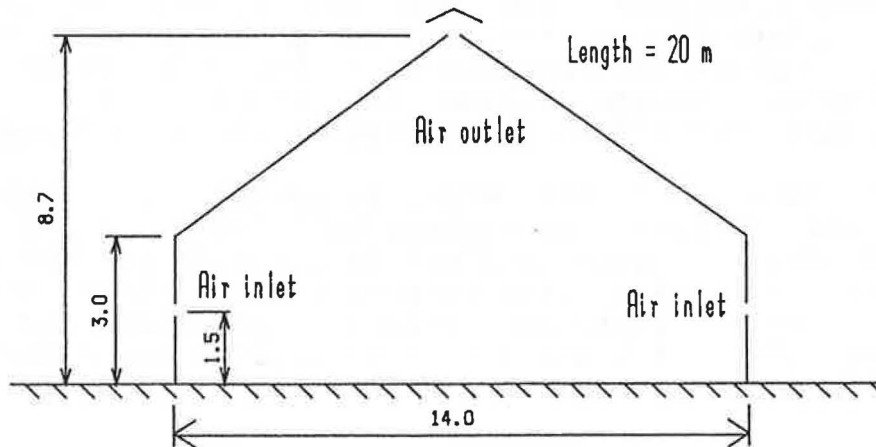


Figure 1 : Experimental sheep-fold of the University of Liège.

Though no similar problem was found in the literature, a general background provided means to analyse test results. In a first approach, jets are often assumed free and isothermal. Jets theory (1, 2) produces a complete velocity profile determined from a selected number of experimental parameters.

Anisothermy between jet and environment creates a deflection of the jet path, usually described as a power law of the distance and as a function of the Archimede number (3). There appears, though, a quite large dispersion of results in the literature.

Jets confinement in space also influences their pathway. Low pressure appears between the jet's boundaries and nearby solid surfaces, thus producing deflection, referred to as the "Coanda effect". In general, the jet path is described by a circle line (4), whose curvature is very dependant upon the geometry.

The study of jets in confined spaces has been the object of many investigations. In residential applications, Jackman (5), Nielsen (6), Brugger (7) are among basic contributors in both experimental and numerical analyses. For industrial or agricultural large spaces, works by Satoshi (8) and Leonard (9) should be mentioned. A special quote should be made of the work of Randal (10), which presents many similarities with our problem, though differences such as the location of air inlets do not allow direct comparisons.

Experimental Analysis and Measurement Techniques

Reduced Scale Model and Similitude

Figure 2 shows a cross section of the model. It represents a slice of the prototype sheep-fold at a scale 1/3. Results could however be extrapolated to other buildings at different scales.

For visualisation purposes, the model was constructed in transparent plexiglas. The upper part of the roof is not similar to the triangular vertex of the prototype. This change of geometry enables the movement of a trailer carrying temperature and velocity sensors inside the model. This modification, however, does not affect air movements in the occupancy zone.

Ventilation in the model is mechanical. Fans exist at inlets and outlets, to control both flowrates and pressure in the model and consequently limit infiltrations. The whole model is located inside a climate room to control its environment. Air inlets present different velocity profiles and turbulence intensity ($TI = 9\%$ and 3.5%) to analyze the effect of those parameters on jets paths.

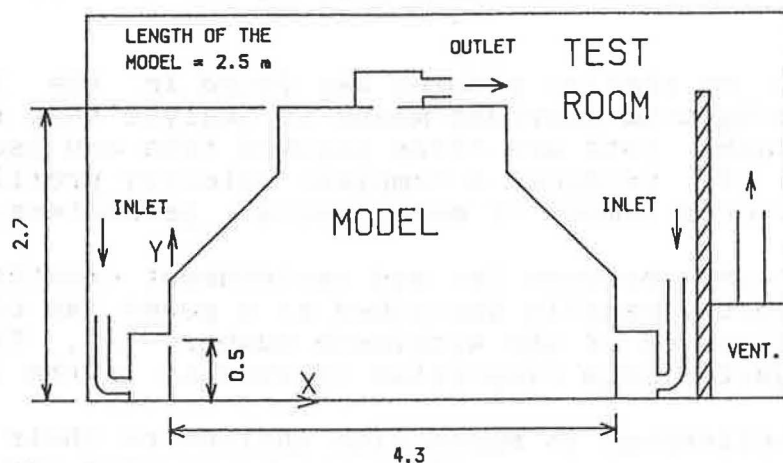


Figure 2 : Cross section of model

Previous observations (11, 8, 9) have shown that similitude criteria must primarily respect the Archimede number (based on inlets characteristics) :

$$Ar_m = Ar_p ,$$

as long as the model Reynolds number remains above a critical value that will actually be determined :

$$Re_m > Re_c$$

Similitude at the boundaries should be fulfilled by the respect of similar geometries and heat transfers. This last condition is very difficult to satisfy properly and local similitude only is applied : walls and laminar boundary sub-layers are excluded from the modelled zone. This implies that heat transfer ratios through any two walls should be respected. This condition is approached by maintaining non heated surfaces at a temperature very close to the mean indoor air temperature and by heating only one (or two) wall(s) at a temperature well above.

Heating is produced by electrically heated panels on the floor. Similar panels are used on the roof to simulate heat loads due to solar radiations.

Instrumentation

Temperatures are recorded by copper-constantan thermocouples. 33 surface temperatures are available, measured on copper plates (5 X 5 cm²). 29 fixed air temperatures are measured in the median test plane and along inlets and outlets. Sensors are shielded thermocouples. Therefore, temperatures are estimated with a confidence interval of ± 0.2 °C. This includes radiation effects, voltage and reference temperature errors.

Air velocities are measured by a spherical, omnidirectional probe TSI 1620. The time constant of the sensor is 2 s (manufacturer value).

The confidence interval associated to air velocity measurements depends upon :

- voltage measurement error;
- directionality of flow;
- natural convection due to the heated sensor;
- integration time to express mean values in a highly turbulent flow.

To evaluate the influence of the integration time, sample preliminary measurements were performed. In various locations of the model, air velocities were continuously recorded over a long period (1/2 hour). Then, mean values were computed on subintervals of time ranging between 10 and 360 s. Typically, the error σ_v is proportional to the standard deviation SD and

decreases with the integration time as $t^{-0.5}$ (12). As the standard deviation can be linearly related to the mean velocity V (13), the error becomes here :

$$\frac{\sigma_v}{V} = 0.43 \left(\frac{1}{t} \right)^{0.5} \quad (1)$$

as illustrated by figure 3.

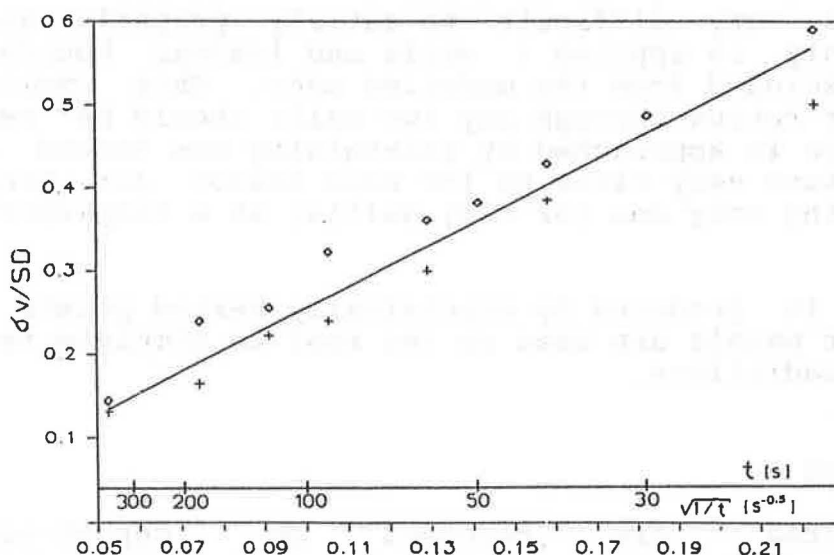


Figure 3 : Error variations with integration time

Measurement values were eventually integrated over a period of 4 minutes, yielding a relative error of 2.8 %. This integration time was reduced to 2 minutes in zones of low velocities, where the overall measurement error is already large and is not much affected by the integration time anymore. In that case, a relative error of 3.9 % is accepted.

Gathering all aspects of the measurement errors, the following values are estimated :

$$\sigma_v = 0.06 V \quad \text{for } V > 0.2 \text{ m/s and 2-D flow}$$

$$\left. \begin{array}{l} \sigma_v = (0.03 + 0.053 V) \\ \text{or } - (0.03 + 0.2 V) \end{array} \right\} \quad \text{for } V < 0.2 \text{ and } 240^\circ \text{ solid angle}$$

$$\sigma_v = 0.11 V \quad \text{for } V > 0.2 \text{ m/s and } = 240^\circ \text{ solid angle}$$

Finally, let us note that the turbulence intensity at the air inlet was recorded with a DISA low velocity anemometer 55D80/81, with a frequency response of 90 Hz.

Test Procedures

Measurements intend to study the effect of the following parameters on the jet position in the model :

- Archimede number (Ar),
- Ratio of velocities at opposite inlets : $F_v = \frac{V_1}{V_2}$,
- Turbulence intensity at inlets TI,
- Relative length of inlets = $\frac{l}{L}$,
- Location of heat sources,
- Location of air exhaust (roof or opposite wall).

Measurements are performed at some 200 various locations in the median plane of the model. 2-D flow is assumed and verified before and after each test by smoke visualisation in different cross sections. Steady state conditions are maintained and regularly verified by fixed point measurements showing an average drift of 0.12°C, with a maximum observed at 0.3°C.

Air Flow Patterns

Figures 4. (a through d) show air flow patterns observed in the model for different ventilation conditions. Figure 4.a is typical of one air inlet of unit relative length (l/L) = 1. The pattern was obtained in presence of distributed heat sources on the floor, but a similar picture is observed when $Ar = 0$. In this geometry, $l/L = 1$ creates a closed zone of air between the jet and the floor where entrainment by the jet creates an underpressure. When the jet strikes the floor, a portion of the volume flow re-enters the subzone to balance the entrainment effect. The resulting deflection of the jet (Coanda effect) is actually increased by Archimede effect if heat sources are present.

When the relative length of the inlet slot is decreased $l/L < 1$, the subzone is now fed by air flowing transversally on the sides and underpressure is no more experienced. When $Ar = 0$, the flow of figure 4.b is observed where the jet flows quite horizontally into the model. In the presence of heat sources, however, deflection occurs and a picture close to figure 4.a is again observed. The location of heat sources (along floor or roof) has no influence on the jets paths in the occupancy zone.

Figure 4.c illustrates a situation where 2 jets enter the model with a high value of the Archimede number ($Ar = 0.01$). Here again, the location of heat sources does not affect flow patterns in the occupancy zone. For low Archimedes, the flow changes drastically, with one jet flowing downwards and the other one upwards (figure 4.d).

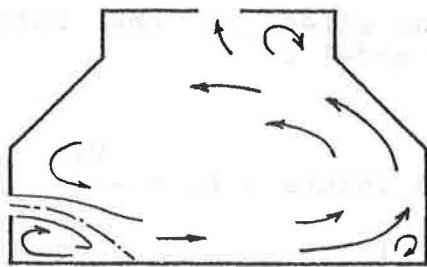


FIGURE 4.A $I/L=1$

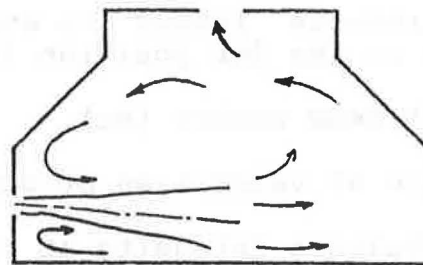


FIGURE 4.B $Ar=0$ $I/L<1$

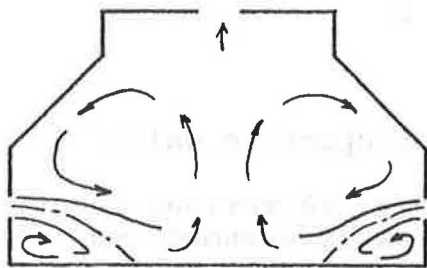


FIGURE 4.C Ar LARGE

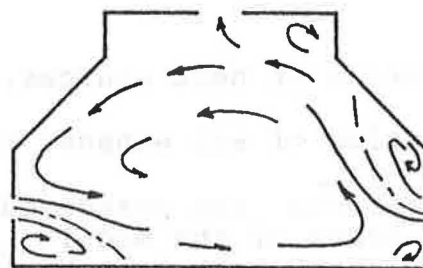


FIGURE 4.D Ar LOW

Figures 4 : Air flow patterns in model

Flows occurring when two jets interact are difficult to predict because specific combinations of parameters may create very unstable situations (figure 4.c or 4.d ?). Unstable flows are described in the literature. They may result from hysteresis phenomena (14) or from bi-stable situations in a geometry strictly symmetrical with respect to the jet inlet (2). In almost all cases, the Coanda effect is responsible for the unstable phenomenon. In our cases, it is combined to the interaction of opposite jets (15).

Actually 3 phases may be observed. First (phase A), each jet develops independantly and the general pattern of flow is represented by figure 4.c. Then (phase B), one jet slightly slips above the other. This phase can be very short in time and could not be analyzed. Finally, a stable phase C can be observed, where one of the jets is deflected towards the roof (figure 4.d).

In some cases, phase A is observed during a quite long period. It happens for a wide range of Ar values and low velocity ratios F_v (figure 5, group I). On the other hand, large ratios F_v correspond to the dominance of one jet's momentum upon the flow. This situation yields the development of phase C in a very short time. Those cases are represented as group III on figure 5. In between (low Ar and low F_v) an unpredictable zone remains. Those cases are represented by group II on figure 5.

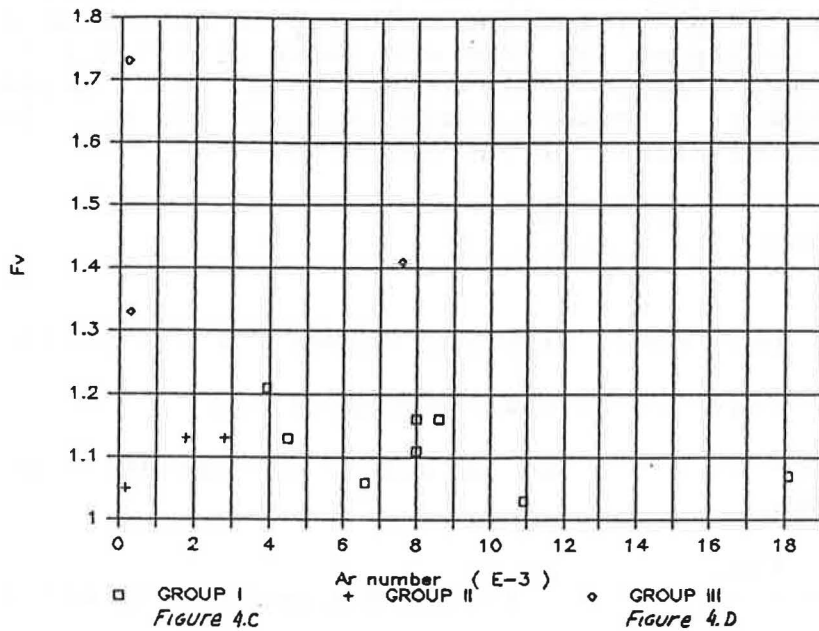


Figure 5 : Classification of air flow patterns with respect to Ar and F_v

In general, the jet with the largest momentum is deflected downwards. The situation may, however, differ if both jets do not initiate simultaneously. Figures 6.a and b show two successive representations of the flow where the jet on the right enters a flow already established by the jet on the left. It is deflected towards the roof by the overall air circulation and further by a Coanda effect along the roof, even when its inlet velocity surpasses by far the other one. This situation illustrates the difficulties encountered to predict air movements in natural ventilation conditions, where wind effects are essentially variable in time.

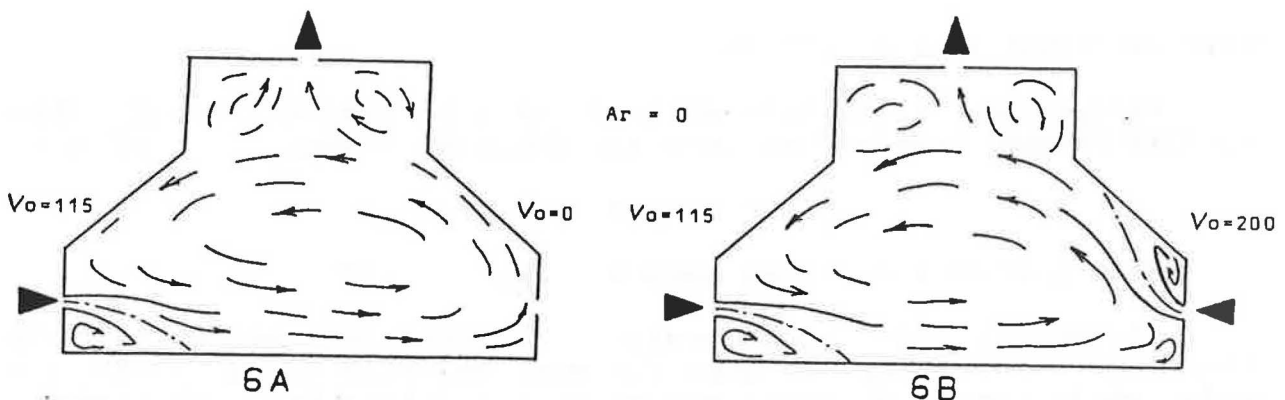


Figure 6 : Air jet entering an established air flow

Jet Location in the Occupied Zone

Jets will be localized by the position of their central line, i.e., the locus of maximum velocity in any cross section. At successive distances (x) from the inlet (x > 0.2 m to avoid the initial core zone), velocities have been measured at different heights y_1 . Assuming Gaussian velocity profiles (and neglecting the local effect of curvature) :

$$V_1 = V_m \exp \left(- \frac{y_1 - y_m}{C} \right)^2 ,$$

interpolation is performed, yielding values for V_m , y_m and C.

Further restrictions to this procedure are :

- $y_1 > 0.15$ m to avoid the influence of jets impingement on the ground;

- $\left(\frac{V_{\max} - V_{\min}}{V_{\max}} \right) > 0.1$ to yield a reasonable error on y_m in case of very flat velocity profile.

For comparison purposes with available results in the literature, the jets pathways will be considered as circle lines in isothermal conditions but as power laws if the Archimede effect is dominant.

Independance from the Reynolds Number

For $l/L = 1$ and $Ar \approx 0$, the jet path is a circular arc. By regression, its curvature radius has been determined for various Reynolds numbers between 1200 and 4500 (figure 7). This yields a correlation law for the radius :

$$R = 1.64 + 7.03 (\text{Re} \times 10^{-3})^{-5.24} \quad (\text{m})$$

with an error $\sigma_x = \pm 0.29$ (m).

Evidently, similitude criteria will be respected only when results become independant from the Reynolds number, i.e. when :

$$R < 1.64 + \sigma_x$$

This yields a critical number : $\text{Re}_c = 1850$

Obviously, the consideration of other parameters as the turbulence intensity or even the mean velocity at a reference point would result in other values of a critical Reynolds number. The present approach seems, however, adequate for the analysis of jets deflections.

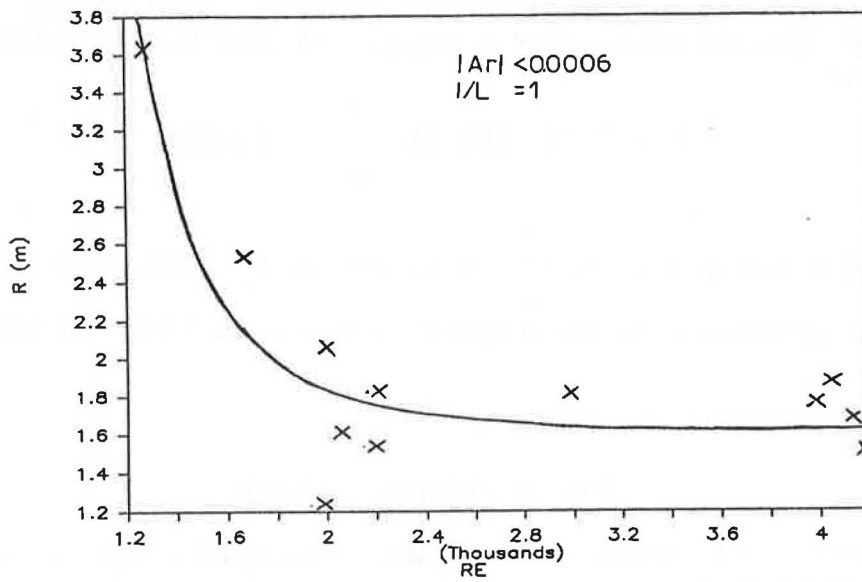


Figure 7 : Curvature vs Reynolds number
($l/L = 1$, $|Ar| < 0.0006$)

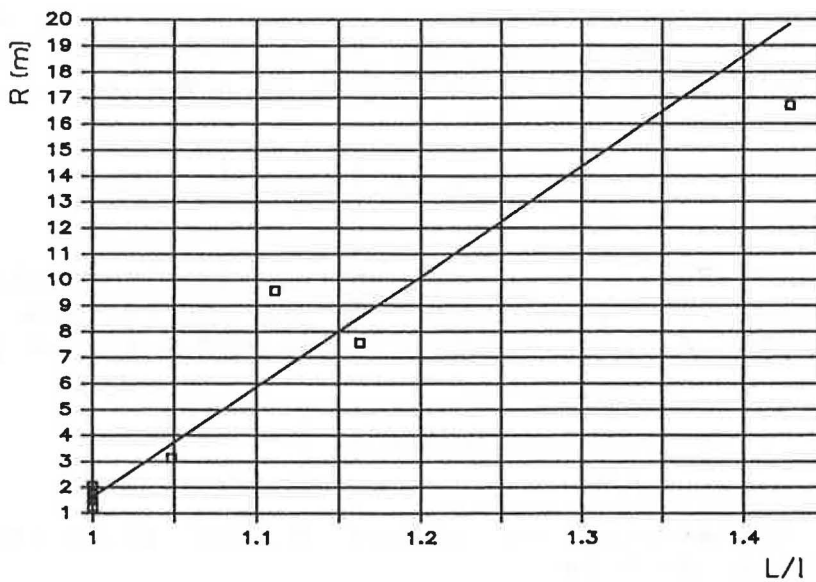


Figure 8 : Curvature vs. relative length L/l)

Influence of Relative Length of Slots (1/L)

Observations (figures 4.a and b) have already revealed the importance of the ratio 1/L on the jets curvature. Figure 8 confirms this statement for several isothermal tests in similitude conditions ($Re > Re_c$). It can be expressed by the correlation :

$$R = 1.64 \left(25.86 \frac{1}{L} - 24.86 \right) \quad (m)$$

valid in the range $0.7 \leq \frac{1}{L} \leq 1$. Actually lower values of $\frac{1}{L}$ present no interest as no significant deflection is observed.

The Archimede Effect

Effects of anisothermy are analyzed by means of the Archimede number :

$$Ar = \frac{g \beta (T_x - T_o) b_o}{V_o^2}$$

Where T_x is the mean temperature of the air, b_o the width of the inlet and V_o is defined by

$$V_o = \frac{1}{b_o} \left[\int_0^{b_o} u^2 (y) dy \right]^{0.5}$$

Here $u(y)$ represents the velocity profile at the inlet.

Experiments show that the Coanda effect is dominated by the anisothermy, whenever $1/L < 0.86$. In that situation, the central line of the jet is generally described by a power law such as :

$$\frac{Y}{b_o} = C Ar \left[\frac{x}{b_o} \right]^n$$

Koestel (3) suggests an exponent $n = 3$. In practice, lower values are generally encountered. In our application, a value of 2.5 was observed. A correlation on measurement points yields :

$$\frac{Y}{b_o} = 0.366 Ar \left[\frac{x}{b_o} \right]^{2.5}$$

It is illustrated on figure 9 for situations in the similitude range ($Re > Re_c$)

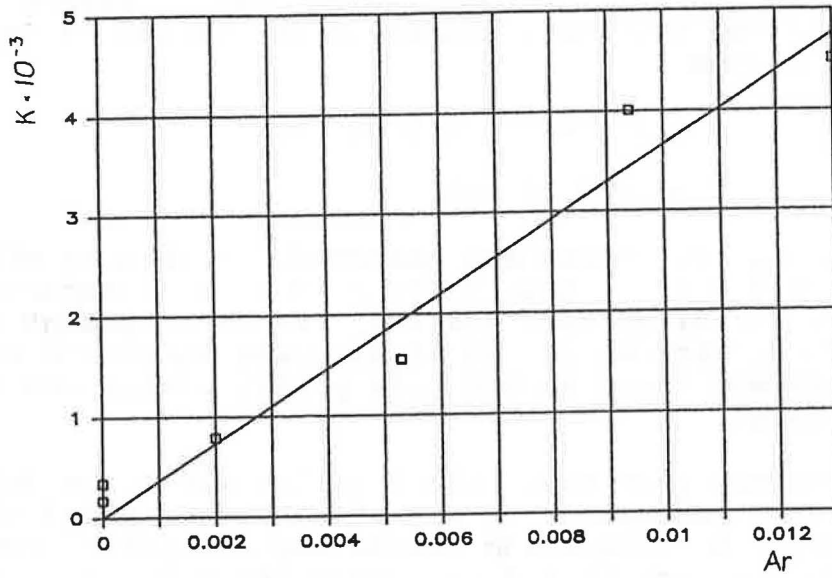


Figure 9 : Anisothermy effect

$$K = C Ar = \frac{y b_o^{3/2}}{x^{5/2}}$$

$1/L \leq 0.86$ and $Re > Re_c$

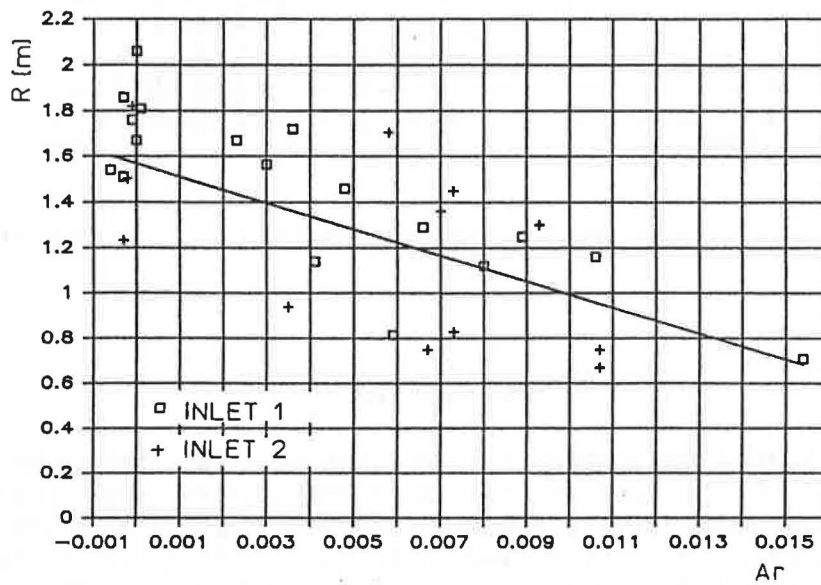


Figure 10 : Curvature vs Archimede number for $1/L = 1$ and $Re > Re_c$

Coanda and Archimede Effects Combined

When both Coanda and Archimede effects are combined, we tried to represent jets paths by circular arcs. Figure 10 shows the influence of the Archimede number on its radius of curvature, yielding a regression :

$$R = 1.64 - 66.0 \text{ Ar (m)}$$

$$\sigma_x = 0.27 \text{ (m)}$$

On figure 10, all tests are gathered, combining effects of inlet 1 (TI = 3.5 %), inlet 2 (TI = 9.0 %), separately or simultaneously, floor or roof heating, exhaust through the roof or through the opposite wall. No significant influence of any of those parameters was found on the jets paths, within the accuracy of our experiments.

For comparison purposes, the location where the jet enters the occupancy zone (assumed at $y = 0.25 \text{ m}$) was computed with both approaches (only Ar effect and Coanda and Ar effect combined). They happen to agree for $\text{Ar} \geq 0.06$, where the ratio l/L ceases to influence the path of the jet (figure 11).

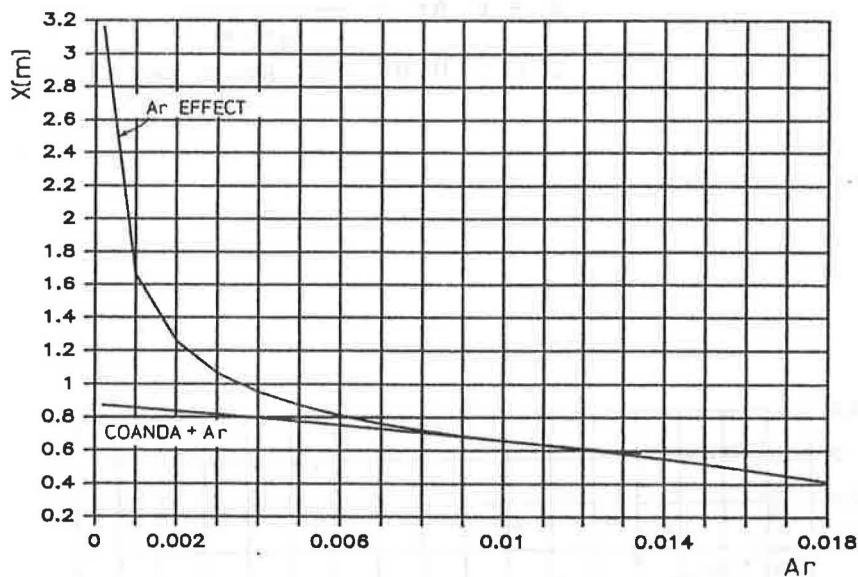


Figure 11 : Location where the jet enters the occupancy zone

Discussion

For the specific geometry considered, we can conclude that the most important parameters influencing the jets paths in the occupancy zone are the Archimede number, the relative length of the ventilation slots (l/L) and the ratio of inlet velocities F_v . Other factors such as turbulence intensity at the inlets or location of exhaust have not been found significant, with respect to the dispersion of our results.

The radius of curvature of the jet seems unaffected by the number of jets entering the model, though the establishment of the air flow pattern is highly affected by the number of jets and their relative momentum. Also, the location of heat sources (roof or floor) has indeed local effects but does not affect the jets paths in the occupancy zone.

Jets deflections under the Archimede effect, described by the power law are in good agreement with available literature (2, 3, 16). Coanda effects in isothermal flow are seldom found in the literature. Comparison with Bourque's experiments (4) shows large differences up to 37 %. Half of that range can be explained by differences in methodology, where Bourque locates the jets impingement on the floor by pressure measurements. The other half (considering a 7 % error on the radius of curvature) could be explained by secondary effects such as recirculation, jets location fluctuation or 3-D behaviour.

A cattle shed was selected as prototype building. Those often experience natural ventilation. Fluctuations in wind intensity and direction create a quite large spectrum of inlet conditions and it seems of interest to determine how often the conditions analyzed here are encountered in reality. Measurements on the prototype building during 10 days of winter provide hints on the subject based on about 3000 sets of measurements. Figures 12 and 13 show the cumulated frequency of occurrence of the Reynolds and Archimede numbers. We can observe that 95 % of the measurements present a Reynolds number above the critical value of 1850 and that the range of Ar considered in the present work occurs about 50 % of the time ($Ar < 0.02$). For larger Archimede numbers, natural convection is likely to become dominant in the building and air movements may differ drastically.

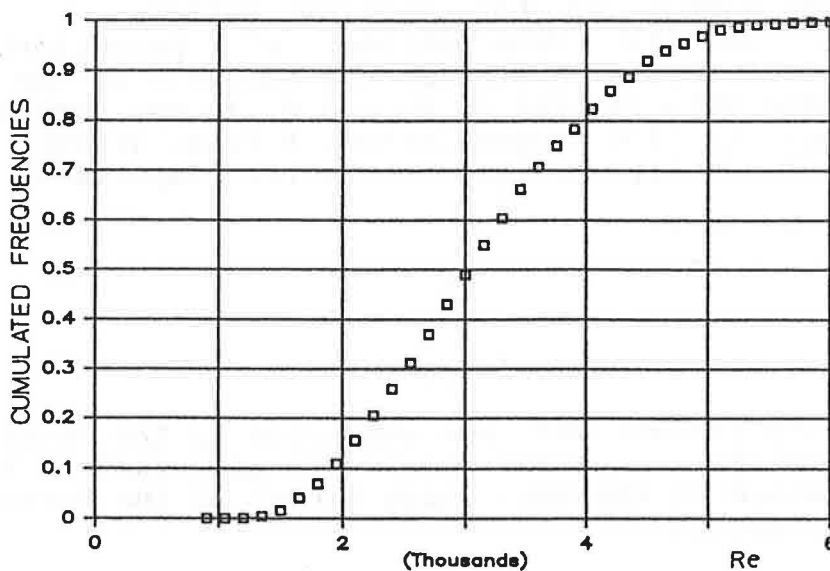


Figure 12 : Cumulated frequencies of Re in the prototype building

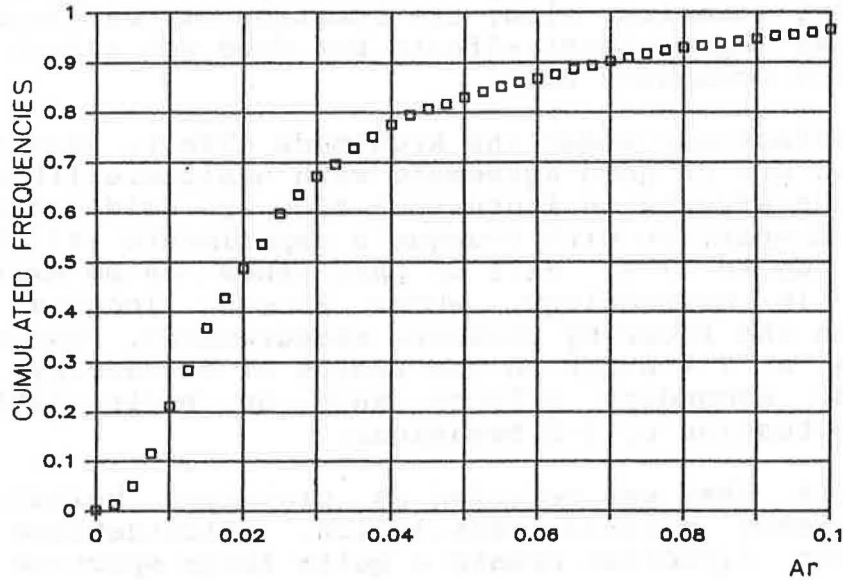


Figure 13 : Cumulated frequencies of Ar in the prototype building

Conclusion

Once flows are established, jet paths in the occupancy zone of the building may be represented by quite simple formulations. The dominant parameters influencing those paths are the Archimede number, the relative length of the ventilation slots and the ratio of inlet velocities in opposite slots.

The establishment of the airflow pattern is however crucial, and certain combinations of parameters yield unpredictable situations. A statistical analysis of the various flows encountered with respect to Ar and F_v in the unstable range seems appropriate to lift uncertainties. A first attempt has been done here, but mostly to demonstrate the importance of the problem.

Acknowledgements

Part of the present work was supported by the Faculties of Agronomy of Gembloux. Special thanks are addressed to Professor Nicks and Mr Canard of the Veterinary School of the University of Liège for their advice.

References

- (1) Abramovich, G.N. The Theory of Turbulent Jets. The Massachusetts Institute of Technology. 1963.
- (2) Baturin, B.B. Fundamentals of Industrial Ventilation. Pergamon Press, Oxford, 1972.
- (3) Koestel, A. Paths of Horizontally Projected Heated and Chilled Air Jets. ASHRAE Trans, 1955, 61, 213-233.
- (4) Bourque, C. Newman, B.G. Reattachment of a Two-dimensional Incompressible Jet to an Adjacent Flat Plate. The Aeronautical Quarterly, Vol. XI, August 1960.
- (5) Jackman, P.J. Holmes, M.J. Designing for Satisfactory Air Distribution in Rooms. Clima 2000, Milan, Vol. 2, 1975.
- (6) Nielsen, P.V. Measurements on Buoyant Wall Jet Flows in Air Conditioned Rooms. ROOMVENT-87, Stockholm, 1987.
- (7) Brugger, P. Kegel, B. Displacement Ventilation for an Office Building with Triple Glazed Windows. Clima 2000, Sarajevo, 1989.
- (8) Satoshi, T. Scale Model Experiment of Air Distribution in the Large Space of the Shinkokuikan Sumo Wrestling Arena. ROOMVENT-87. Stockholm, 1987.
- (9) Leonard, J.J. McQuitty, J.B. The Use of Archimedes Number in the Design of Ventilation Systems for Animal Housing. Conference on Agricultural Engineering. Adelaide 24-28 August, 1986.
- (10) Randall, J.M. Battams, V.A. Stability Criteria for Airflow Patterns in Livestock Buildings. J. Agric. Eng. Res., 1979, 24, 361-374.
- (11) Mierzwinski, S. Some Experiences in Air Distribution Research. Internal Communication. Technical University of Gliwice, Poland.
- (12) Launder, B.E. Spalding, D.B. Mathematical Model of Turbulence. Academic Press. London. 1972.
- (13) Hanzawa, H. Melikow, A.K. Fanger, P.O. Airflow Characteristics in the Occupied Zone of Ventilated Spaces. ASHRAE Trans., 93.1, 1987.
- (14) Nielsen, P.V. Restivo, A. and Whitelaw, J.H. Buoyancy Affected Flows in Ventilated Rooms. Numerical Heat Transfer, 1979, 2, 115-127.
- (15) Fissore, A. Experimental Determination of the Position of Jets for Slot Ventilated Spaces. Proc. of Air Flow Patterns in Ventilated Spaces. Liege, Belgium. February, 1989.
- (16) Croome, D.J. Air Conditioning and Ventilation of Buildings. Gale & B.M. Roberts, 1975.

